



Therapeutic Efficacy Of Curcuma And Pomelo Loaded Chitosan Nanoparticles In Intestinal Murine Trichinellosis

Wafaa Fayez Abd El-Hamed^a, Ahmed A. Abd-Rabou^{b*}, Asmaa Antar Faramawy^c

^a Biological and Environmental Sciences Dept., Faculty of Home Economics, Al-Azhar University, Egypt

^b Hormones Department, Medical Research and Clinical Studies Institute & Stem Cell Laboratory, Center of Excellence for Advanced Science, National Research Centre, 12622, Giza, Egypt.

^c Nutrition and Food Science Dept., Faculty of Home Economics, Al-Azhar University, Egypt.



CrossMark

Abstract

The majority of the medications used to treat trichinellosis had little bio-availability and a elevated resistance level. This work compared the usage of Curcuma longa extract, pomelo peels extract, and their chitosan (CS) nanoparticles (NPs) versus the existing albendazole treatment for experimental trichinellosis. A total of 49 male albino mice were used in this study. Healthy controls (GI), infected untreated controls (GII), Albendazole-treated infected group (GIII), infected group receiving pomelo peels extract (IV), infected group receiving pomelo peels extract-loaded CS NPs (GV), infected group receiving Curcuma longa extract (GVI), infected group receiving Curcuma longa extract-loaded CS NPs (GVII). They were divided into seven experimental groups: healthy control (GI), infected untreated control (GII), Albendazole administered infected group (GIII), infected group receiving pomelo peels extract (IV), infected group receiving pomelo peels extract-loaded CS NPs (GV), infected group receiving Curcuma longa extract (GVI), and infected group receiving Curcuma longa extract-loaded CS NPs (GVII). The extracts were given orally to experimentally infected mice at a rate of 100 mg/kg/day commencing 24 hours after infection and continuing for 14 days on parasite burden, histological alterations in the gut, skeletal muscle, and oxidative stress. Except for the healthy control group, all groups were infected orally with *T. spiralis* larvae at a dose of 200 larvae per mouse. On the 35th day following infection, all groups were sacrificed. The results demonstrated a significant reduction in adult worm count during the intestinal phase in all treated groups. The group treated with pomelo NPs had the highest reduction rate of adult worms, at 94.13 %. For the group treated by pomelo NPs, it showed better rank compared to non-infected group and albendazole administered infected group, as well as reduced larval count during muscle phase, the highest reduction rate of larvae was 80.2% for the group treated by Curcuma NPs. The same concept has been counted for the encysted phase. This was reflected further by improved parasite burden, histopathological alterations, cytokines and oxidative stress compared to control group and Albendazole administered infected group. TNF- α , IL-6, NOS2, SOD3, α -GST concentrations have been investigated in sera and showed that TNF- α , IL-6, and NOS2 levels have been elevated significantly ($P < 0.01$) in infected group (GII), while SOD3 and α -GST levels have been significantly decreased compared to negative control (GI) ($P < 0.01$). Treatment of infected mice with Curcuma and pomelo NPs have been significantly improved ($P < 0.05$) all parameters levels in sera and back them close to the original levels of negative control. Finally, we can conclude that introduction of Curcuma and pomelo NPs could be of therapeutic potential use against trichinellosis.

Key words: Trichinella spiralis, Albendazole, Chitosan Nanoparticles, Curcuma longa, pomelo peels.

1. Introduction

Trichinellosis is a dangerous zoonotic parasite illness that is found all over the world. [1]. The intestinal phase of trichinellosis is crucial since it dictates both the disease's course and outcomes. The public risk caused by these larvae in human ingestion is linked to their distribution load in different muscles. Because trichinellosis is so widely spread among carnivorous animals, consumers must take extra care to avoid becoming infected [2]. Humans contract the virus by eating meat from pigs or other

animals that have been infected with Trichinella larvae. These larvae are released from capsules after eating infected meat, invading the intestinal cells at the top position and maturing to adult worms. They are fertilised in 2–3 weeks. Females yield 1500 newborn larvae, which enter and encapsulate in the skeletal muscles *via* lymphatic and blood systems [3]. The Trichinella larvae persuade the muscle cell to develop into a new one, known as a nurse cell, which allows the larvae to live for months to years [4]. The treatment for *T. spiralis* that is now available is

*Corresponding author e-mail: ahmedchemia87@yahoo.com; (Ahmed A. Abd-Rabou).

Receive Date: 23 October 2021, Revise Date: 02 December 2021, Accept Date: 11 November 2021

DOI: 10.21608/EJCHEM.2021.102400.4750

©2022 National Information and Documentation Center (NIDOC)

ineffective [5]. The major anthelmintic medications used to treat trichinellosis are benzimidazole analogues like albendazole (ABZ) and others [6]. Despite this, they have a low bioavailability, a high risk of resistance, and only moderate action against encapsulated muscle larvae [7]. Furthermore, several of these medications are prevented for pregnant women as well as the under 3 children [8], while others are thought to be carcinogenic [9]. As a result, efforts must be performed to recuperate effective and safe antitrichinellosis medications using plants as medicines [8], where they have low toxicity and minimum burden effects [10].

Pomelo (*Citrus grandis* L. Osbeck) is a popular citrus fruit endemic to the moderate tropical regions of Southeast Asia. The fruits and peels are high in Vitamin C and antioxidants such as β -carotene, β -sitosterol, polyphenols, and others [11]. Anti-inflammatory, anti-oxidant, and anti-microbial features are all found in pomelo. Pomelo peel oil (PPO) is high in antioxidants [12].

Curcumin, the major active element in *Curcuma longa* L., has been demonstrated to have many pharmacological advantages, including anti-parasitic actions [13]. Curcuma is high in antioxidants, anti-inflammatory, anti-infection, and anti-tumor compounds. Curcumin possesses many pharmacological activities. This compound has anti-oxidant, anti-inflammatory, anti-infectious, anti-viral, and anti-carcinogenic impacts [14]. It reduces the burden of parasite worm, pathology, and granuloma size in the afflicted hepatic cells [13]. Curcumin has been used as encapsulated NPs because it is a powerful, biocompatible, and bioactive substance with antibacterial properties [15].

Chitosan nanoparticles (CS NPs) have been utilized as a drug delivery approach for the cryptosporidium therapy [16]. Previous researches have employed NPs as vehicles to deliver medications to improve the effectiveness of therapy [17]. Infections can affect healthy hosts, while also stimulating the immune system of the infected host. The immune system responds by producing harmful oxidants known as free radical species [18].

Biochemical parameters, such as nucleic acid, proteins, carbohydrates, lipids, and micro-nutrients including vitamins, and carotenoids have been definitely proven to be damaged by "radicals" [19]. Reactive oxygen species (ROS), for instance hydroxyl and superoxide radicals, as well as hydrogen peroxide are responsible for cell mortality [20].

Chronic inflammation, age-related illnesses, and cancer are all linked to ROS [21]. Because free radicals are at the heart of many disease pathways, lowering their production or completely eliminating

these chemical species could be beneficial for disease prevention and treatment [22]. Many anti-oxidants in cells modulate the ROS formation, including enzymatic and non-enzymatic processes [20], which enable them to neutralise ROS, to defend biological organisms from free radical damage [23].

Antioxidant enzymes like as catalase (CAT), superoxide dismutases (SODs), glutathione reductase (GR), as well as glutathione peroxidases (GPxs) are part of the complex endogenous antioxidant system [24]. Non-enzymatic substances such as glutathione (GSH) [25] also play an important role. By conjugating ROS and detoxifying lipid peroxidation products, GSH shields the cell from the harmful effects of endogenous and external oxidants [26,27,28]. Interleukin-6 (IL-6) and IL-1 are expressed constitutively in human myoblasts, whereas IL-1 and tumour necrosis factor (TNF- α) are only found following treatment with pro-inflammatory cytokines. IL-6 is a multifunctional cytokine that is released in response to tissue injury and infections [28,29].

Nitric oxide (NO) plays a limited function in the evacuation of *T. spiralis* adults during the intestinal phase of *T. spiralis* infection, but it is mostly involved in intestinal pathology [30]. Many structural and metabolic changes occur in muscles during the muscular phase, which are modulated by ROS (nitrogen and oxygen radicals) released from the parasite and its host. These ROS can be reacted with NO to generate peroxy-nitrate, which causes muscle fibre mortality. This elevated iNOS activity in *T. spiralis*-infected mice's skeletal muscle may play a role in the host's biochemical defence mechanism [30].

Overall, the goal of this work is to examine the effects of Pomelo and Curcuma extracts and their CS NPs on oxidative stress, parasitological, and histopathological parameters in mice infected with Trichinellosis in an experimental models.

2. Materials and methods

Experimental animals

This study was conducted on 49 laboratory-bred female Swiss albino mice that were purchased from Theodor Bilharz Research Institute, Imbaba, Giza, Egypt, housed and fed according to the national guidelines, the experiment has been approved by the Research Ethics Committee.

Extraction of methanolic pomelo peels and curcuma longa extracts

For preparing the extracts, the method of Ojarudi's group [31] was used with some modifications (pomelo peels and rhizome of curcuma longa) was

obtained from the local market at the Tanta governorate, Egypt. Each Curcuma longa rhizome or dreid pomelo peels was ground with a mechanical grinder into a fine powder. The 200 g of powder was dissolved in 600 ml of 95% ethanol in a beaker and then kept in a water bath for 2 h at 50°C following filtration and with whatman No. 1 filter paper more than once and it was dried at room temperature.

Preparation of the inoculums

The diaphragms of heavily diseased pigs were chopped into small pieces and manually combined. Artificial digestion fluid (1 percent pepsin, W/V & 1 percent HCL, V/V) was used to digest these fragments. Larvae were collected using the Baermann technique in phosphate buffered saline at the end of the digestion process [32]. The number of larvae per ml. solution was calculated after the sediment of larvae was separated in clean petri-dishes and washed with phosphate buffer saline [32].

Parasite and dose of infection

Mice were prevented from food 12 hours before infection, then each mouse was received 200 orally inoculated larvae using a tuberculin syringe with blunt nozzle according to [33].

Preparation of curcuma and pomelo extracts-loaded chitosan nanoparticles

The electrostatic interaction between negatively and positively charged molecules such as poly anionic and cationic polymers is used to create nanoparticles (NPs) via the ionotropic gelation process. The amino groups on chitosan NPs linked with anionic groups of TPP salt in curcuma or pomelo extract-encapsulated chitosan NPs. TPP was synthesised at 1 mg/mL in acidified distilled water (DW), and chitosan mixture was conducted at 1 mg/mL in DW. To begin, 1 mL of chitosan mixture was agitated for 10 minutes before being adjusted to 1.5 mL with DW. Then, to 1 mg/mL of Kumquat extract, add 5 L tween 80. The extracts of curcuma and pomelo were then added to the chitosan mixture in two distinct tubes. Finally, 100 µL of TPP solution as a cross linker were added to emulsified-Curcuma or pomelo extract-chitosan solution in a dropwise way. The obtained solution was stirred for 30 min and centrifuged at 4000 g for 5 min. At last, the supernatant was transferred into a new tube and kept for subsequent analysis [34].

Curcuma and pomelo extracts-loaded chitosan NPs characterization

The samples were sonicated for 5 min before being analyzed and they were immediately used for measurements.

Entrapment efficiency measurement

Dialysis tubing technique was used to purify the synthesized NPs for eliminating the impurities and the free non-conjugated compounds suspended in the solution by eluting it through regenerated cellulose (Amicon 10,000 MWCO ultra filter, Millipore, USA). The Entrapment efficiency (EE%) for the NPs were measured and processed with the microplate reader (BMG Labtech, Germany). The compound entrapment efficiency was calculated from the ratio of the compound amount incorporated into the NPs to the total added compound amount [35].

Transmission electron microscopy (TEM)

Particle morphology of the NPs was examined by TEM (Philips CM-10, FEI Inc., Hillsboro, OR, USA). 100 µg/mL of the NPs were dropped into formvar-coated copper grids, and after complete drying, the samples were stained using 2% w/v uranyl acetate (Electron Microscopy Services, Ft. Washington, PA). Image capture and analysis was done using Digital Micrograph and Soft Imaging Viewer Software [36].

Particle size and zeta potential analyses

Particle size and zeta potential of the NPs were determined using Malvern Zeta Sizer (Nano ZS, Malvern Instruments, UK). All the samples were maintained at a constant temperature of 25.0°C.

Study design groups of animals

This study was carried out on laboratory bred Swiss albino male mice (n = 49) aged 8 weeks, weighing 20–25 g. Stool examination of the mice was done prior to the study to sure the absence of any intestinal parasitic infection.

All mice in the studied groups except normal control were infected with *T. spiralis larvae*. The experimentally mice were classified into seven main groups (7 mice /cage) where they were categorized into the following groups; GI: non-infected and non-treated (negative control); GII: infected and non-treated (positive control); GIII: infected, treated with Albendazole drug; IV: infected, treated with curcuma longa extract V: Curcuma longa extract-loaded CSNPs, GVI pomelo peels extract and GVII pomelo peels extract-loaded CSNPs.

The infected mice (GIII - GVII) were treated orally starting from first day PI by Albendazole (ABZ) drug (GIII) or with 50mg/kg of tested extracts twice daily (GIV to GVII) for 14 successive days. On the 7th and 30th days post-infections, the infected mice were sacrificed by their neck dislocation.

Albendazole administration

Albendazole (ABZ) drug was purchased from the Egyptian International Pharmaceutical Industries Co.

One tablet (100mg) was dissolved in 50ml distilled water and given orally in a dose of 50mg/kg/day for three consecutive days [37].

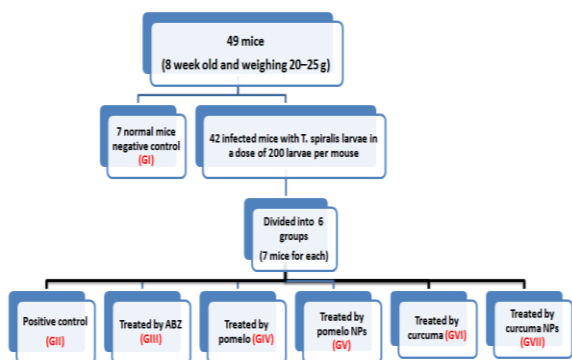


Fig. 1: Flow chart of experimental design

Parasitological Examination

For counting the number of adult worms, four mice from each infected groups (untreated and treated infected groups) were sacrificed on the 7th day to investigate the effects of the extracts and their NPs against adult worms (intestinal phase) [38]. Small intestines of the treated and untreated infected groups were removed, opened longitudinally were cut into 2 cm pieces and placed in a beaker containing 250 ml 0.85% physiological saline at 37°C for 3–4 h. After that, the intestine was shaken well in the solution and rinsed with saline. All the fluid was collected and centrifuged at 1500 rpm for 5 min. The worms were counted in the reconstituted sediment drop by drop using a stereo microscope [39]. The average number of adult worms per mice was also calculated [40]. Moreover, the efficacy of drug group or tested extract groups calculated according to the equation:

$$\text{Efficacy \%} = \frac{A-B}{A} \times 100$$

Where: A = Number of worms or larvae extracted from control animals. B = Number of worms or larvae extracted from treated animals.

Compression diagnostic method

At 30 day all mice were sacrificed, then a piece from each mouse diaphragm was placed between two slides and pressed to obtain a thin layer which was examined under low-power objective to detect the presence of *T. spiralis* larvae and confirm infection [41].

Collection of larvae

Artificial Digestion method

The carcasses of mice were weighed, diced, and digested in acid pepsin solution after evisceration

[42]. Digestion took place at 37°C for 2 hours. Larvae were subsequently separated from each mouse's digest by filtration. Through two layers of gauze onto a 200 mesh cm⁻² sieve [43], which kept any undigested tissues but allowed for digestion the passage of larvae of *T. spiralis*. After that, the tissues were rinsed. Using tap water and simple sedimentation to concentrate larvae 30 minutes technique The supernatant was poured away, and the sediment was left behind and repeatedly cleaned three times with tap water sedimentation.

Counting of *T. spiralis* larvae

The silt was measured, and three 0.1 mL samples were distributed on a microscope slide to count larvae using a McMaster counting chamber (10 objective) [43,37]. We calculated the number of larvae per gram of tissue by averaging the results of three counts. The effectiveness of each formula was determined by comparing the number of larvae collected from infected groups that had been treated and those that had not been treated.

Biochemical analysis

Assessment of oxidant/antioxidant status in sera of mice was evaluated using some ELISA kits of Tumor necrosis factor-alpha (TNF-α), Interleukin 6 (IL-6), Nitric oxide synthase-2 (NOS2), Superoxide Dismutase 3 (SOD3), α-glutathione S-transferases (α-GST) concentrations were quantitatively measured using ELISA kits purchased from (Wuhan Fine Biotech Co., China).

Sample Collection and Storage

The whole blood sample was placed at room temperature for 2 hours and centrifuged for 20 minutes at approximately 1000×g. The serum was collected and the assay carried out immediately. The blood collection tubes were disposable, non-pyrogenic, and non-endotoxin.

ELISA procedure

The Competitive-ELISA detection approach was used in the development of these kits. The target has been pre-coated on the given microtiter plate. During the process, a set amount of target on the solid phase supporter competes with target in the sample or standard for sites on the Biotinylated Detection Antibody specific to target. Excess conjugate and unbound sample or standard were removed from the plate, and each microplate well was incubated with HRP-Streptavidin (SABC). After

that, each well is filled with TMB substrate solution. The enzyme-substrate reaction is stopped, and the colour change is detected using a spectrophotometer at 450nm. The target concentration in the samples is then determined by comparing the OD of the samples to the standard curve.

Histopathological examination

Muscle specimens were acquired from the hind leg of mice euthanized on the 30th dpi, whereas one centimetre from the jejunum at the junction of the proximal 1/3 and distal 2/3 was removed from mice sacrificed 7 dpi [44]. These specimens were fixed in 10% buffered formalin, cut into 1 cm thick slices, dehydrated with alcohol, cleaned with xylol, and then imbedded in paraffin wax, which was then processed into paraffin blocks. Serial paraffin slices of 5m thickness were cut with a Reichert Rotary microtome and stained with Harries Hematoxylin and Eosin [45].

Statistical analysis

All results were presented as mean \pm standard deviation (SD). Results were analyzed statistically by one-way analysis of variance (ANOVA) using SPSS 15.0 program, IBM Company (NY, USA) and value of $P < 0.05$ was considered statistically significant.

3. Results

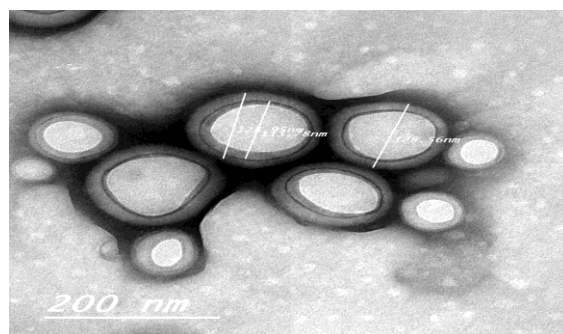
Characterization of the NPs

In the present study, TEM used to illustrate the morphology of the synthesized Curcuma and pomelo extracts-loaded CS NPs. Fig 2A,B showed the TEM images of the two NPs. The average size of the Curcuma NPs was around 127.5 nm (Fig 2A), while the average size of the pomelo NPs was ranging from 137 nm and 247.7 nm (Fig 2B) of the particles in the TEM images. The images display spherical NPs with a nano-capsule of CS shell. The dialysis tubing approach was used to determine the entrapment efficiency (EE %) of synthesised Curcuma and pomelo NPs. The EE percent of the free Curcuma and pomelo inside the nano-capsules was found to be 88.32 % and 91.21 %, respectively (Table 1).

The Curcuma and pomelo-loaded CS NPs were characterized using the Malvern Zeta Sizer equipment Dynamic Light Scattering (DLS). Statistical analysis showed that their Z-average diameters were 125.5 \pm 6.12 nm and 185.84 \pm 9.01 nm, respectively. The polydispersity indexes (PDI) were 0.1 and 0.35 for both NPs, respectively. These results reflect the high constancy of the Curcuma and pomelo NPs. On the surface of the Curcuma and pomelo-loaded CS NPs, there was a constant pattern

of positively charged zeta potential (ZP; + 34.1 \pm 2.51 mV and + 26.5 \pm 7.24 mV, respectively) (Table 1).

A]



B]

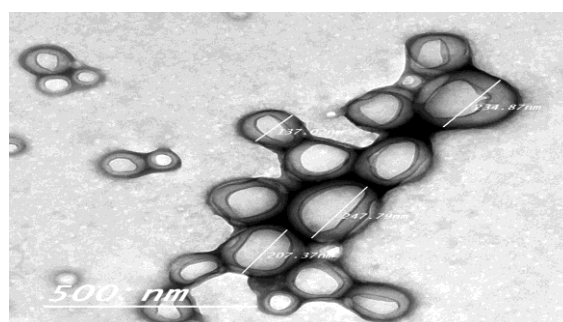


Fig. 2: TEM images of the Curcuma (A) and pomelo (B)-loaded CS NPs. This image showed the morphology of the NPs.

Table (1): Average of size, polydispersity index (PDI), Zeta potential (ZP), and entrapment efficiency (EE) of the synthesized NPs.

The nano-formulation of the Curcuma and pomelo-loaded CS NPs was very stable; where zeta potential and PDI index of the synthesized NPs indicated that they are stable formulations. Because the ZPs were not near to zero and the PDI value was less than 0.5 for both NPs, electrostatic stabilisation would be sufficient to stabilize the suspensions.

Biochemical measurements

ELISA technique was utilized to investigate some factors in mice's sera. TNF- α , IL-6, NOS2,

NPs type	Mean \pm SD			EE, %
	Size, nm	PDI	ZP, mV	
Curcuma NPs	125.5 \pm 6.12	0.1 \pm 0.00	+ 34.1 \pm 2.51	88.32
Pomelo NPs	185.84 \pm 9.01	0.35 \pm 0.01	+ 26.5 \pm 7.24	91.21

SOD3, α -GST levels were tested, and illustrated in

Figs. 3 and 4. In infected group (GII), TNF- α , IL-6, and NOS2 (Fig. 3A,B) levels were elevated significantly ($P < 0.01$), while SOD3 and α -GST (Fig. 4A,B) concentrations were significantly decreased when compared to negative control (GI) ($P < 0.01$).

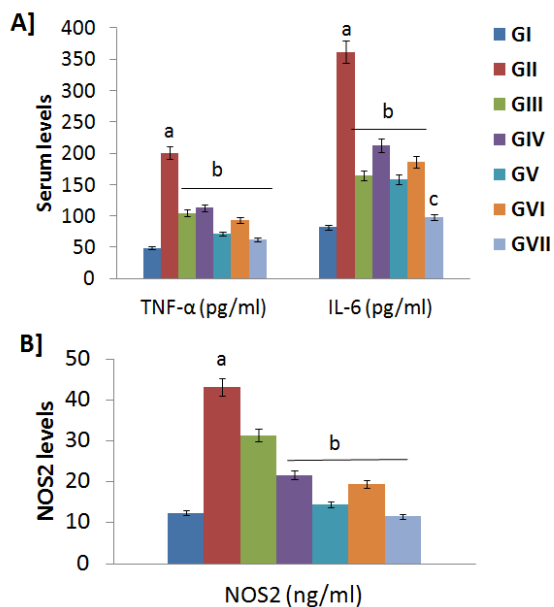


Fig. 3: TNF- α , IL-6 (A) and NOS2 (B) sera levels upon treatments versus positive control (GII) and negative control (GI). a; means significance difference ($P < 0.01$) when comparing GII with GI. b; means significance difference ($P < 0.05$) when comparing treated groups with GII. c; means high significance difference ($P < 0.05$) when comparing treated groups with GII.

Treatment of infected mice with Curcuma and pomelo-loaded CS NPs were significantly improved ($P < 0.05$) all parameters levels in sera and back them close to the original levels of negative control. Indeed, the TNF- α , IL-6, and NOS2 levels in the treated mice with ABZ, Curcuma extract, pomelo extract, and their nanocomposites were significantly decreased ($P < 0.05$) compared to the infected mice group (GII), reporting the highest significant decrease ($P < 0.01$) in GVI.

On the other hand, the SOD3 and α -GST concentrations in the treated mice with ABZ, Curcuma extract, pomelo extract, and their nanocomposites showed high significant increase ($P < 0.01$) compared to the infected mice group (GII), recording significant increase ($P < 0.05$) of SOD3 when comparing GIII and GIV with GII.

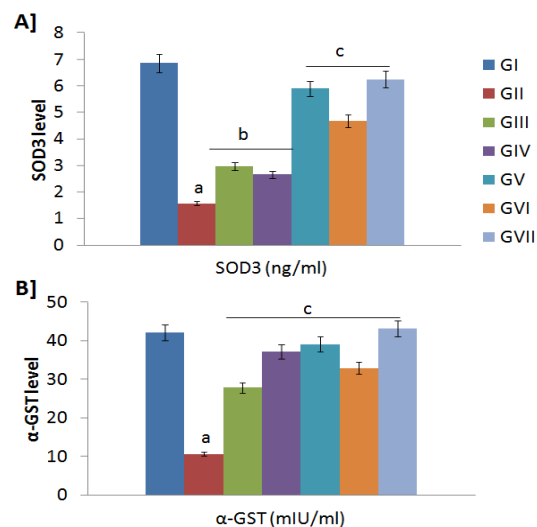


Fig. 4: SOD3 (A) and α -GST (B) sera levels upon treatments versus positive control (GII) and negative control (GI). a; means significance difference ($P < 0.01$) when comparing GII with GI. b; means significance difference ($P < 0.05$) when comparing treated groups with GII. c; means high significance difference ($P < 0.05$) when comparing treated groups with GII.

Effects of pomelo, curcuma, and their NPs against adult worms

A significant reduction of *T. spiralis* adult worm count and larval count was recorded in all treated groups as compared to infected group (G11). There was a significant difference between all treated groups (GII-GVII) ($P < 0.05$). There was a significant difference between albendazole treated group (G111) and all treated groups ($P < 0.01$). The least count was found in group (GV) which received pomelo CS NPs, with efficacy of 94.1% followed by GVII which received Curcuma extract loaded CS NPs with efficacy of 88.26%, followed by (GVI) which received Curcuma extract with efficacy of 74.57%. The least decrease in the adult worms' count has been seen in pomelo-treated group (GIV) with efficacy of 56.96% (Table 2).

Effects of extracts and their NPs against encysted larvae

On day 30 after infection, there was a significant decrease of total larval counts in the infected treated group ($44 \pm 0.81, 6 \pm 0.81, 26 \pm 1.82, 12 \pm 1.63$) in groups (GIV-GVII) as compared with infected untreated group (68.75 ± 4.78) ($P < 0.05$), with resistance to infection 0%. The best reduction of larval count was found in groups (GV and GVII) which received pomelo peels extract loaded CS NPs and Curcuma CS NPs with resistance to infection

79.9%, followed by GVI which received Curcuma extract with resistance to infection 67.63%. The least decrease in the count of the average larva has been seen in pomelo-treated group (GIV) with resistance to infection with efficacy 50.54%.

Table (2): Effects of extracts and their NPs against adult worms

Groups	Intestinal worms (Mean±SD)	Resistance to infection %
GI	0	Not infected
GII	102.25 ^a ±1.7	-
GIII	0 ^b	100
GIV	44 ^b ±0.81	56.96
GV	6 ^b ±0.81	94.13
GVI	26 ^b ±1.82	74.57
GVII	12 ^b ±1.63	88.26
Sig. (P<0.05)	0.00	-

a; means significance difference (P <0.01) when comparing GII with GI. b; means very high significance difference (P =0.00) when comparing treated groups with GII.

Table (3): Effects of extracts and their NPs against encysted larvae

Groups	muscle larvae (Mean±SD)	Resistance to infection %
A	0	Not infected
B	68.75 ^a ±4.78	-
C	0 ^b	100
D	34 ^b ±2.94	50.54
E	20 ^b ±2.16	70.9
F	22.25 ^b ±2.87	67.63
G	20 ^b ±0.81	70.9
Sig (0.05)	0.00	-

a; means significance difference (P <0.01) when comparing GII with GI. b; means very high significance difference (P =0.00) when comparing treated groups with GII.

Histopathological changes

Histopathological changes in the small intestinal sections of different experimental groups (H&E at high power view X (200 ×, 400 ×) (Figs. 5-11). Normal group (G1) showed normal small intestinal structure, and no histopathological changes were observed (Fig. 5). Infected control group (GII): Intestinal wall showed thin mucosal thickness with markedly and totally necrotic villi, partially necrotic crypts, moderate inflammatory infiltrate with scattered eosinophils extending to underlying submucosa and musculosa (Fig. 6).

Albendazole (ABZ) treated group (GIII): Intestinal wall showed average mucosal thickness with average villi/crypt ratio, villi with average connective tissue cores, intact brush border and average goblet cells, average crypts, average submucosa, as well as average musculosa (Fig. 7).

Pomelo extract treated group (GIV): Intestinal wall showed scattered fragmented and partially necrotic villi, villi with edematous connective tissue cores, partial loss of brush borders and depletion of goblet cells, average crypts, average submucosa, as well as average musculosa (Fig.8).

Pomelo loaded CS NPs (GV): Intestinal wall showed scattered fragmented and partially necrotic villi with viable intra-mucosal parasite, villi with average connective tissue cores, preserved brush borders and average goblet cells, scattered fragmented and necrotic calcified crypts, submucosa with mild inflammatory infiltrate, and partially edematous musculosa (Fig. 9).

Curcuma extract group (GVI): Intestinal wall showed few scattered partially necrotic villi, scattered villi with edematous connective tissue cores, marked lymphoid hyperplasia, crypts with scattered apoptotic cells, average submucosa, as well as average musculosa (Fig. 10).

Curcuma extract loaded CS NPs group (GVII): Intestinal wall showed marked decrease of mucosal thickness with intra-mucosal parasites, partially necrotic villi, totally necrotic crypts with mild inflammatory infiltrate and mildly dilated congested blood vessels, as well as average musculosa (Fig. 11).

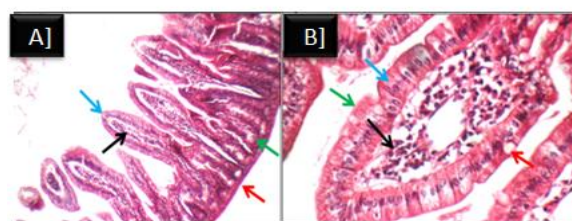


Fig. 5: Normal control (GI). A) high power view of intestinal wall showing average villi/ crypt ratio and villi composed of connective tissue core (black arrow) covered by tall columnar epithelial cells (blue arrow), average crypts (green arrow), and average musculosa (red arrow) (H&E X 200). B) higher power view showing average villi composed of connective tissue core (black arrow) covered by tall columnar epithelial cells (blue arrow) with intact brush border (red arrow) and average goblet cells (green arrow) (H&E X 400) .

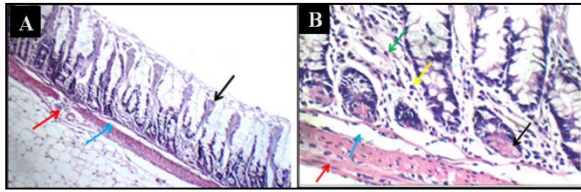


Fig 6: positive control group (GII). A) high power view of intestinal wall showing thin mucosal thickness with markedly necrotic villi (black arrow), average submucosa (blue arrow), and destructed musculosa with mild inflammatory infiltrate (red arrow) (H&E X 200). B) another view showing partially necrotic crypts (black arrow), moderate inflammatory infiltrate (yellow arrow) with scattered eosinophils (green arrow), average submucosa (blue arrow), and average musculosa (red arrow) (H&E X 400).

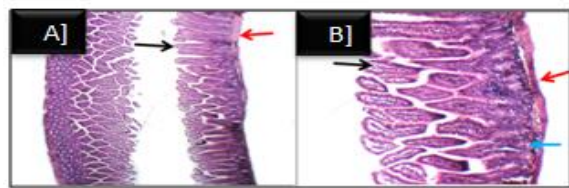


Fig 7: drug control group (GIII). A) intestinal wall showing average mucosal thickness with average villi (black arrow), and average musculosa (red arrow) (H&E X 100). B) high power view showing average villi/ crypt ratio with average villi (black arrow), average crypts (blue arrow), and average musculosa (red arrow) (H&E X 200).

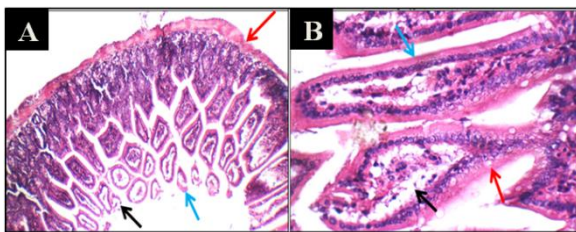


Fig. 8: Pomelo extract group (GIV). A) another view of intestinal wall showing scattered fragmented (black arrow) and partially necrotic villi (black arrow), and average crypts (red arrow) (H&E X 200). B) higher power view showing villi with edematous connective tissue core (black arrow), partial loss of brush borders (blue arrow) and depletion of goblet cells (red arrow) (H&E X 400).

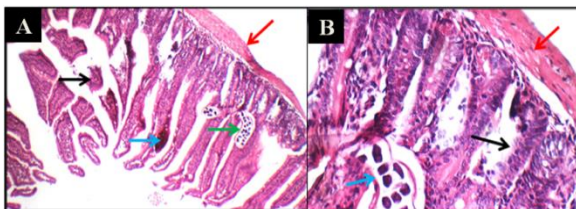


Fig. 9: Pomelo extract loaded CS NPs group (GV). A) high power view of intestinal wall showing scattered fragmented (black arrow) and partially necrotic villi (blue arrow), intra-mucosal parasite (green arrow), and average musculosa (red arrow) (H&E X 200). B) another view showing fragmented crypts (black arrow) with viable intra-mucosa parasite (blue arrow), and partially edematous musculosa (red arrow) (H&E X 400).

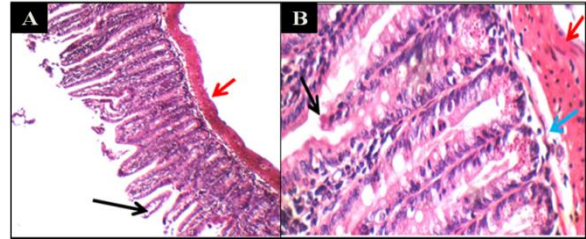


Fig.10: curcuma extract group (GVI). A) high power view of intestinal wall showing scattered villi with edematous connective tissue cores (black arrow), and average musculosa (red arrow) (H&E X 200). B) another view showing crypts with scattered apoptotic cells (black arrow), average submucosa (blue arrow), and average musculosa (red arrow) (H&E X 400).

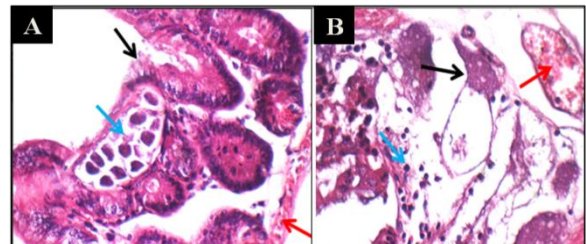


Fig. 11: curcuma extract loaded CSNPS group (GVII). A) higher power view of intestinal wall showing partially necrotic villi (black arrow) with intra-mucosal parasite (blue arrow), and average musculosa (red arrow) (H&E X 400). B) higher power view showing partially necrotic crypts (black arrow) with mild inflammatory infiltrate (blue arrow), and mildly dilated congested blood vessels (red arrow) (H&E X 400).

Histopathological changes in the skeletal muscle sections of different experimental groups (H&E at high power view X (200 ×, 400 ×) represented in (Figures 12 - 18). Normal group (GI): showed normal muscle cells with no inflammatory reaction (Fig. 12).

Infected control group (GII) showed skeletal muscle showed heavy infestation by viable parasites with mild inflammatory infiltrate, and partially necrotic muscle fibers (Fig. 13). Albendazole (ABZ) treated group (GIII) skeletal muscle showed partially edematous and markedly necrotic muscle fibers, with few scattered inflammatory infiltrate, and no parasites (Fig.14). Pomelo treated group(GIV): skeletal muscle showed heavy infestation by viable parasites, some parasites are partially calcified, marked inflammatory infiltrate, lymphoid hyperplasia, and markedly necrotic muscle fibers (Fig. 15). Pomelo loaded CS NPs showed skeletal muscle showed few scattered partially necrotic muscle fibers, no parasites (Fig 16). Curcuma extract group skeletal muscle showed heavy infestation by viable parasites and ova, marked inflammatory infiltrate, and scattered partially necrotic muscle fibers (Fig. 17). Curcuma CS NPs group showed skeletal muscle showed heavy infestation by viable and few scattered necrotic parasites with marked inflammatory infiltrate, and partially necrotic muscle fibers (Fig. 18).

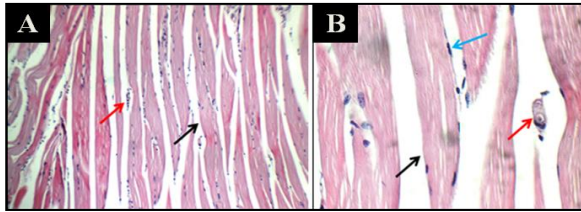


Fig 12: Normal control (GI). A) skeletal muscle showing average muscle fibers with distinct borders (black arrow), and average interstitium (red arrow) (H&E X 200). B) high power view showing average muscle fibers with distinct borders (black arrow) and peripherally located nuclei (blue arrow), and average interstitium with average blood vessels (red arrow) (H&E X 400).

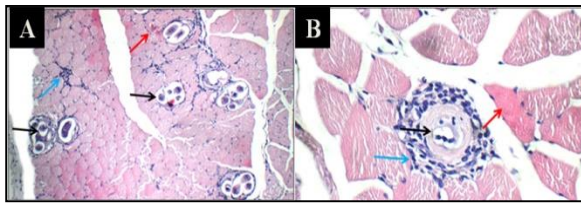


Fig 13: positive control group (GII). A) skeletal muscle showing heavy infestation by viable parasites (black arrow) with mild inflammatory infiltrate (blue arrow), and partially necrotic muscle fibers (red arrow) (H&E X 200). B) high power view showing viable parasite (black arrow) with mild inflammatory infiltrate (blue arrow), and partially necrotic muscle fibers (red arrow) (H&E X 400).

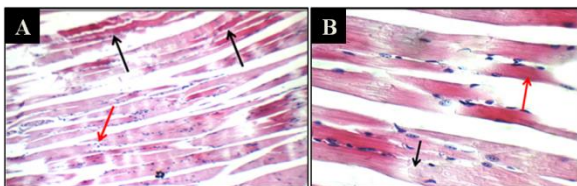


Fig. 14: Drug control group (GIII). A) high power view of skeletal muscle showing markedly necrotic muscle fibers (black arrow), and few scattered inflammatory infiltrate (red arrow), no parasites (H&E X 400). B): another view showing partially edematous (black arrow) and partially necrotic muscle fibers (red arrow), no parasites (H&E X 400).

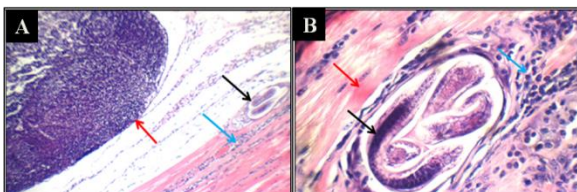


Fig. 15: pomelo extract group (GIV). A) skeletal muscle showing infestation by viable parasites (black arrow) with marked inflammatory infiltrate (blue arrow), and lymphoid hyperplasia (red arrow) (H&E X 100). B) another view showing partially calcified parasite (black arrow) with marked inflammatory infiltrate (blue arrow), and partially necrotic muscle fibers (red arrow) (H&E X 400).

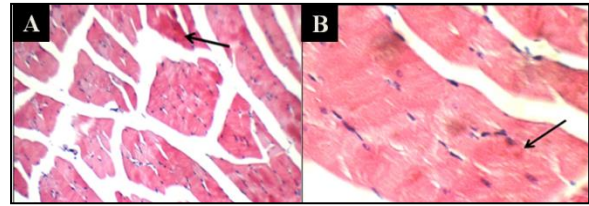


Fig 16: pomelo loaded CSNPS group (GV). A) high power view of skeletal muscle showing few scattered partially necrotic muscle fibers (black arrow), no parasites (H&E X 200). B) higher power view showing few scattered muscle fibers with bright eosinophilic cytoplasm (black arrow), no parasites (H&E X 400).

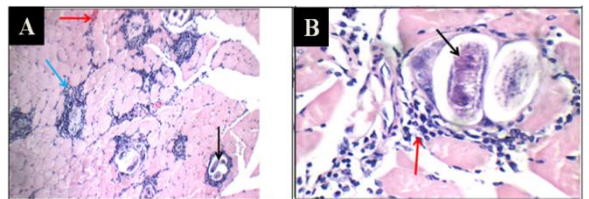


Fig 17: curcuma extract group (GVI). A) high power view of skeletal muscle showing heavy infestation by viable parasites (black arrow) with marked inflammatory infiltrate (blue arrow), and partially necrotic muscle fibers (red arrow) (H&E X 200). B): another view showing infestation by viable parasite (black arrow), and marked inflammatory infiltrate (red arrow) (H&E X 400).

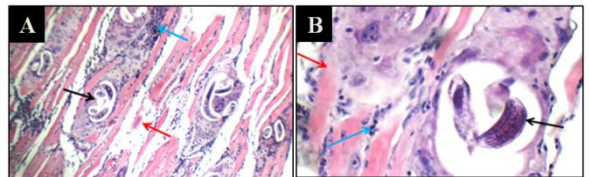


Fig. 18: curcuma loaded CSNPS group (GVII). A) high power view of skeletal muscle showing heavy infestation by viable parasites (black arrow) with marked inflammatory infiltrate (blue arrow), and partially necrotic muscle fibers (red arrow) (H&E X 200). B): another view showing infestation by viable parasites (black arrow) with mild inflammatory infiltrate (blue arrow), and partially necrotic muscle fibers (red arrow) (H&E X 400).

Discussion

Because of its broad spectrum of activity and low cost, albendazole is widely used against intestinal parasites [46]. However, numerous important parameters influence its efficacy, including oral bioavailability, which is mostly determined by solubility, and the timing of treatment initiation after infection [47]. According to several recent studies, there may be a strong chance of finding some alternative medication molecules derived from medicinal plants that can be used to treat *T. spiralis* infections effectively [48,49,50].

The efficiency of pomelo extract, Curcuma extract, and pomelo and Curcuma extract loaded CS NPs against different stages of *T. spiralis* in mice was compared to a positive control and albendazole, a

common commercial medicine. The present study disclosed a remarkable low in the average count of adult worms as well as larvae in all treated groups. ABZ showed the highest effect versus both the intestinal and muscular phases. These results showed high significant decrease in the average count of adult worms in treatment with pomelo extract NPs followed by Curcuma longa extract loaded CS NPs, while curcuma extract then pomelo extract had the least efficacy. While pomelo and Curcuma extract loaded CS NPs had the same effect on larvae count (70.9%) reduction followed by Curcuma extract then pomelo extract Tables (2 and 3).

These findings corroborated those of [46], who stated that micro-crystals prepared from CS seem to be the best choice for optimising the absorption of compounds orally. They also stated that microencapsulated formulations (based on chitosan particles of various concentrations) were designed to improve albendazole dissolution rate in treating *T. spiralis* infected mice during the intestinal pharyngitis phase.

The high therapeutic response was related to improved albendazole bioavailability and intestinal bioavailability in these formulations, as well as improved drug dissolution rate and, as a result, drug absorption by intestine *T. spiralis* w. These results agreed with Priotti's group [46] who indicated that the micro-crystals made with CS appear to be the best options to optimize oral absorption of the active reported that microencapsulated formulations based on CS particles with different concentrations, designed to improve albendazole dissolution rate in treating *T. Spiralis* infected mice during the intestinal phase of the parasite cycle. The high therapeutic response observed was due to a better bioavailability of albendazole and improvement of the intestinal bioavailability of the drug in these formulations and improving the drug dissolution rate and consequently, its absorption by intestinal *T. spiralis* worms. The smaller the particle size, the higher the surface area and the faster the dissolving rate of drug particles is well-known [46].

Abdel-Latif's team [51] found that chitosan particles reduced both adult and egg counts in mice infected with *H. nana* (95 % for adult and 77 % for eggs).

The current findings contradicted with that mentioned by Gaafar's team [52], who found no significant reduction in parasite count in the infected group treated with chitosan nanoparticles in the treatment of murine toxoplasmosis when compared to controls. When compared to the free medication, curcumin-loaded nanoparticles demonstrated less cytotoxicity. As a result, CS-coated NPs could be a promising technique for directly delivering curcumin

into the oral cavity for the treatment of oral cancer [53]. Treatment with *C. maxima* peel extracts has the potential to be both therapeutic and immunoregulatory in the treatment of Cryptosporidiosis [54].

A significant reduction in the present study in serum TNF- α on 30th days p.i. was observed in all treated groups (GIII- GVII) compared to positive control (GII). Curcuma CSNPs (GVII) showed the highest reduction, followed by group treated with pomelo extract CS NPs (GV), followed by groups treated with Curcuma extract and pomelo extract, respectively. TNF- α is implicated in apoptosis and systemic inflammation. Wu's team found that the TNF- α /TNF receptor 1 signalling pathway is involved in nurse cell production *via* apoptosis and anti-apoptosis [55], with associated indirectly with our findings.

IL-6 is the first myokine to be discovered, and it is secreted by muscle cells to regulate metabolic processes in other tissues [56]. IL-6 production from exercised muscle was linked to a high plasma IL-6 content [57]. It was found IL-6 gene expression in *T. spiralis*-infected people' peripheral blood mononuclear cells treated with crude worm extract. These findings show that elevated IL-6 expression in diseased skeletal muscle can contribute to systemic IL-6 induction, which has been described as a pro-inflammatory cytokine as well as an anti-inflammatory myokine [58].

T. gondii [59,60] is an example of an infectious pathogen for which IL-6 is a key cytokine in the protective immune response [61]. They was also found that after *T. gondii* infection and treatment with enrofloxacin, toltrazuril, or a combination of sulfadiazine and pyrimethamine, proinflammatory cytokines such as IL-6 were reduced in villous explants. These findings could be one way for the parasite to elude the immune system, according to the authors.

The immune system's functional role of nitric oxide (NO) is debatable. As a result, the role of NO in parasite diseases is still being debated, and further research is needed [62]. Inducible nitric oxide synthase (iNOS or NOS2) inhibitor aminoguanidine (AG) [63]. It has been utilised in several experimental investigations to examine its effect on parasite load and the inflammatory process, including toxocariasis, filariasis, hymenolepiasis, and strongyloidiasis [64]. iNos oxide in untreated infected mice showed very high significant value compared to infected treated mice. After administration of tested extract, extract loaded CS NPs showed a significant reduction in serum NOS2 on 30th days p.i. GV and GVII in this study revealed a high significant decrease in the NOS2 compared to other groups.

In mice persistently infected with *Toxoplasma gondii*, the iNOS inhibitor L-NMMA (NG-monomethyl-L-arginine) indicated reactivation of infection with enhanced inflammatory alterations in brain regions, according to Scharton-Kersten et al. [65]. In contrast to previous findings [66], it was discovered that iNOS activity is not required for the regulation of intra-cerebral persistent toxoplasmosis in the latent phase of infection. Mice infected with toxoplasmosis and treated with the L-N6-iminoethyl-lysine (L-NIL) iNOS inhibitor revealed decreased iNOS expression in brain regions [67].

SOD, GPx, and TAS are antioxidant enzymes that help the body fight free radicals [68]. SOD and GPx are two of the most important defence antioxidants, preventing the formation of new free radical species by converting existing free radicals into less harmful molecules before they can react, or by preventing the formation of free radicals from other molecules. In the present study, we observed a significant increase in the activity of both antioxidant enzymes SOD and GSH in the blood from mice infected with *T. spiralis* and treated with pomelo loaded CS NPs and curcuma loaded CS NPs compared to other groups.

As shown in our results, GSH (non-enzymatic antioxidant or α -GST) decrease in the serum of infected-untreated mice showed oxidative stress in the current investigation. Muscle tissues from infected mice showed a similar increase in SOD activity from mice infected with *T. spiralis* [69].

Our findings imply that antioxidant enzymes like SOD and GPx, as well as non-enzymatic low molecular antioxidants, may play a key role in the host's biochemical defence mechanisms against oxygen-derived free radicals during trichinellosis. The importance of antioxidant processes in host defence mechanisms during parasite infections (*Plasmodium* spp., *Schistosoma mansoni*, *Dicrocoelium dendriticum*, *Wuchereria bancrofti*, *Trypanosoma cruzi*) has been proven in various researches.

Before settling inside the striated muscles, *T. spiralis* can generate systemic inflammatory symptoms throughout the body. During migration, its most deadly stage, new borne larvae (NBL), passes through the bloodstream of several organs [70]. After penetrating skeletal muscle tissue, *Trichinella* larvae cause a strong inflammatory response, which is responsible for the accompanying myopathy [71]. When compared to infected untreated mice, there was a significant reduction in histopathological abnormalities, including the inflammatory cellular infiltration, necrotic muscle fibers and larval deposition. The majority of infected mice treated with the tested extract showed mild inflammation, however animals treated with pomelo and curcuma

loaded chitosan nanoparticles showed the greatest reduction in inflammation and larvae deposition of all the treatment groups. The change in histopathology agrees with Abou Rayia's team [37].

This could be because CS-based microcrystals appear to be the greatest alternative for optimising oral absorption [72]. It was also widely understood that the smaller the particle size, the higher the surface area and the faster the drug particle dissolution rate [46].

Prior investigations found a link between histopathological alterations and previous studies [50,37]. Controlling inflammation lowered the release of systemic cytokines from activated immune cells, alleviating symptoms such as fever, tissue edoema, and vasculitis [29]. Furthermore, Abdel Latif's results have agreed with the current CS findings [51]. In *Hymenolepis nana* infected mice, CS improved intestinal morphometric measures and reverted changes to nearly normal length and width, as well as crypts.

Curcumin has been used in the creation of nanoparticles as a powerful, biocompatible, and bioactive agent with antibacterial properties [16,17]. Curcumin was loaded into chitosan nanoparticles using an ionotropic gelation technique in this work. Citrus peel extracts were found to be efficient against root knot nematodes [73]. Curcumin has been used in the creation of nanoparticles as a powerful, biocompatible, and bioactive agent with antibacterial properties [16,17]. Curcumin was loaded into chitosan nanoparticles using an ionotropic gelation technique in this work. Citrus peel extracts have been shown to be effective against nematodes [73].

Conclusion

The findings of the current study denote that remarkable biochemical, oxidative stress, histopathological, and parasitological alterations may have a therapeutic role for trichinellosis treatment *in vivo* when treated with Curcuma or pomelo-loaded CS NPs.

- Competing of Interests:

The authors declare that there is no conflict of interest.

-Authors Contributions:

AA Abd-Rabou, the corresponding author, synthesized and characterized the nanoparticles. All authors (WF Abd El-Hamed, AA Abd-Rabou, and AA Faramawy) contributed in all biological experiments in this work; mice modelling, parasitology, and histopathology, biochemical, stress markers, and ELISA sections, as well as writing and editing the manuscript.

References

1. Al-Attar T.A.M., El-Kersh W.M., Sadek G. S., Harba N.M., Osheiba S.F. And Brakat R.M.; A Study Of Immunotherapeutic Efficacy Of *Trichinella Spiralis*

- Excretory-Secretory Proteins In Murine Trichinellosis, *Journal of the Egyptian Society of Parasitology*, 50(2), 281 - 292 (2020).
2. Krivokapich S.J., Pozio E., Gatti G.M., Prous C.L., Ribicich M., Marucci G., Rosa G.L. and Confalonieri V. ; *Trichinella patagoniensis* n. sp.(Nematoda), a new encapsulated species infecting carnivorous mammals in South America, *International Journal for Parasitology*, 42(10),903-10 (2012).
 3. Saad A.E., Ashour D.S., Abou-Rayia D.M. and Be-deer A.E.; Carbonic anhydrase enzyme as a potential therapeutic target for experimental trichinellosis, *Parasitol. Res.* ,115, 6, 2331-9 (2016).
 4. Despommier D.D.;*Trichinellida, Diocto-phymatida and Enoplean Parasites*, Ch.23. In:*Foundations of Parasitology*, 8th ed. McGraw-Hill companies, Inc., New York (2009).
 5. Mostafa E. and Atwa H. ;*Intestinal mastocytosis in Trichinella spiralis* infection: immunohistochemical study in murine modele. *Parasitologists United Journal*, 13(1) , 2090-2646 (2020)
 6. Gottstein B., Pozio E. and Nöckler K.; *Epidemiology, diagnosis, treatment, and control of trichinellosis*, *Clin Microbiol Rev.*, 22(1),127-45 (2009).
 7. Codina A.V. ,García A., Leonardi D., Vasconi M., Di D .Masso R.J., Lamas M.C. and Hinrichsen L.I. ; *Efficacy of albendazole:β-cyclodextrin citrate in the parenteral stage of Trichinella spiralis* infection, *Int J Biol Macromol*, 77, 203-6 (2015).
 8. Yadav A.K. and Temjenmongla; *Efficacy of Lasia spinosa* leaf extract in treating mice infected with *Trichinella spiralis*, *Parasitol Res.* ,110(1), 493-8 (2012).
 9. Shalaby M.A. and Moghazy F.M. , Shalaby H.A. and Nasr S.M.; *Effect of methanolic extract of Balanites aegyptiaca* fruits on enteral and parenteral stages of *Trichinella spiralis* in rats, *National Library of Medicine* 107(1),17-25. doi: 10.1007/s00436-010-1827-9. (2010).
 10. Basyoni M.M.A and El-Sabaa A.A.A. ;*Therapeutic potential of myrrh and ivermectin against experimental Trichinella spiralis* infection in mice. *Korean J Parasitol* ,51(3),297-304 (2013).
 11. Ali Y., Rumpa N.N. , Paul S. , Hossen S., Tanvir E. M. , Hossan T., Saha M., Alam N., Karim N. , Khalil I. and Gan S.H. ; *Antioxidant Potential, Subacute Toxicity, and Beneficiary Effects of Methanolic Extract of Pomelo (Citrus grandis L. Osbeck) in Long Evan Rats*, *Journal of Toxicology*, 2019 (2019) <https://doi.org/10.1155/2019/2529569>.
 12. Zou X., Xie L., Wang W., Zhao G., Tian X. and Chen M. ;*Pomelo peel oil alleviates cerebral NLRP3 inflammasome activation in a cardiopulmonary resuscitation rat model*, *National Library of Medicine* , 21(3),233 (2021). doi: 10.3892/etm.2021.9664.
 13. Hussein A., Rashed S., El Hayawan I. El-Sayed R. and Ali H. ; *Evaluation of the Anti-schistosomal Effects of Turmeric (Curcuma longa) Versus Praziquantel in Schistosoma mansoni* Infected Mice, *Iran J Parasitol* ,12(4), 587-596 (2017).
 14. Cheraghipour K., Marzban A., Ezatpour B., Khanizadeh S. and Koshki J.; *Antiparasitic properties of curcumin: A review*, *AIMS Agriculture and Food*, 3(4),561-578 (2018). DOI:10.3934/agrfood.2018.4.561
 15. Bhawana S., Basniwal R.K., Buttar H.S., Jain V.K. and Jain N.; *Curcumin nanoparticles: preparation, characterization, and antimicrobial study*, *J Agric Food Chem.*,59(5),2056-61 (2011).
 16. Pujals G, Suñé-Negre JM, Pérez P, García E, PortusM, Tico JR, Miñarro M, Carrió J. *In vitro* evaluation of the effectiveness and cytotoxicity of meglumine antimoniate microspheres produced by spray drying against *Leishmania infantum*. *Parasitol Res* 102(2008)
 17. Gaafar M.R., Mady R.F., Diab R.G. and Shalaby T.I.; *Chitosan and silver nanoparticles: Promising anti-toxoplasma agents*, *Exp. Parasitol*,143,30-8 (2014).
 18. Saleh M.A., Mahran O.M. and Al-Salahy B.M ;*Circulating oxidative stress status in dromedary camels infested with sarcoptic mange*, *Vet. Res. Commun*, 35, 35-45 (2011).
 19. Alok S., Jain S.K., Verm A., Kumar M., Mahor A. and Sabharwalc M.; *Herbal antioxidant in clinical practice: A review*, *Asian Pacific Journal of Tropical Biomedicine* , 4(1), 78-84 (2014).
 20. Patlevič P., Vašková J., Švorc P., Vaško L. and Švorc P.; *Reactive oxygen species and antioxidant defense in human gastrointestinal diseases*, *Integrative Medicine Research*, 5(4),250-258 (2016).
 21. Zou X., Xie L., Wang W., Zhao G., Tian X. and Chen M. ;*Pomelo peel oil alleviates cerebral NLRP3 inflammasome activation in a cardiopulmonary resuscitation rat model*, *National Library of Medicine* , 21(3),233 (2021).
 22. Sharifi-Rad J., Sharifi-Rad M. , Salehi B. and Iriti M.; *In vitro and in vivo assessment of free radical scavenging and antioxidant activities of Veronica persica* Poir ,*National Library of Medicine* ,64(8),57-64 (2018).
 23. Sánchez C.; *Reactive oxygen species and antioxidant properties from mushrooms* *Synthetic and Systems, Biotechnology* , 2(1),13-22 (2017).
 24. Al-Kayiem A.H.H. and Ibrahim M.A. ;*The influence of the equivalent hydraulic diameter on the pressure drop prediction of annular test section*, *IOP Conf. Ser., Mater. Sci. Eng.*, 100, 012049 (2015).
 25. Forman H.J., Zhang H. and Rinna A. ;*Glutathione: Overview of its protective roles, measurement, and biosynthesis*, *Mol. Asp. Med.*, 30, 1-12 (2009).
 26. Pisoschi A.M. and Pop A. ;*The role of antioxidants in the chemistry of oxidative stress: A review*, *Eur. J. Med. Chem.*, 97, 55-74 (2015).
 27. Kiran T., Karaman U., Arici Y. and Yildiz S. ;*Comparison of malondialdehyde, nitric oxide, adenosine deaminase and glutathione levels in patients with Entamoeba coli, Enterobius vermicularis, Giardia intestinalis, Demodex spp. positive, hydatid cyst and Toxoplasma gondii* serum positive, *Ann. Med. Res.*, 26, 1420 (2019).
 28. De-Rossi M., Bernasconi P., Baggi F., Waal-Malefy R. and Mantegazza R.; *Cytokines and chemokines are both expressed by human myoblasts: possible relevance for the immune pathogenesis of muscle inflammation*, *Int Immunol.*,12,1329-1335 (2000).
 29. Tanaka, T., Narazaki, M., and Kishimoto, T. (2014). *IL-6 in inflammation, immunity, and disease. Cold Spring*

- Harb. *Perspect. Biol.* 6:a016295. doi: 10.1101/cshperspect.a016295
30. Boczon⁷ K., Wandurska-Nowak E., Wierzbiński A., Frydrychowicz M., Mozer-Lisewska I. and Zeromski J.; mRNA expression and immunohistochemical localization of inducible nitric oxide synthase (NOS-2) in the muscular niche of *Trichinella spiralis*. *Folia, Histochem Cytobiol*, 42, 209-213 (2004).
 31. Ojarudi, M., A Moradi, A., Hajhosseini, R., Mazani, M., and Rezagholizadeh, L. (2020): Hepatoprotective and Antioxidant Activities of Combination of *Cinnamomum zeylanicum* and *Zingiber officinale* in CCl₄-intoxicated Rats. *Journal of Kerman University of Medical Sciences*, 2020; 27 (1): 1-130
 32. Dupouy Camel J., Soule C. and Ancelle T.; Recent news on trichinellosis: another outbreak due to horsemeat consumption in France in 1993, *Parasite*, 2, 99-103 (1994).
 33. Dunn I.J. and Wright K.A.; Cell injury caused by *Trichinella spiralis* in the mucosal epithelium of B10A mice, *J. Parasitol*, 71, 6, 757-66 (1985).
 34. Desai, K.G. (2016) Chitosan nanoparticles prepared by ionotropic gelation: An overview of recent advances. *Crit Rev Ther Drug Carrier Syst.*; 33 (2):107-158.
 35. Abd-Rabou, A.A., & Ahmed, H.H. (2017). CS-PEG decorated PLGA nano-prototype for delivery of bioactive compounds: A novel approach for induction of apoptosis in HepG2 cell line. *Advances in Medical Sciences* 62: 357–367.
 36. Abd-Rabou, A.A., Abdelaziz, A. M., Shaker, O.G., & Ayeldeen, G. (2021). Metformin-loaded lecithin nanoparticles induce colorectal cancer cytotoxicity via epigenetic modulation of noncoding RNAs. *Mol Biol Rep.*, In Press, doi: 10.1007/s11033-021-06680-8.
 37. AbouRayia D.M., Saad A.E., Ashour D.S. and Oreiby R.M.; Implication of artemisininematocidal activity on experimental trichinellosis: in vitro and in vivo studies, *International Journal for Parasitology*, 66, 56–63 (2017).
 38. Wang ZQ, Liu RD, Sun GG, Song YY, Jiang P, et al, 2017: Proteomic analysis of *Trichinella spiralis* adult worm excretory-secretory proteins recognized by sera of patients with early trichinellosis. *Front. Microbiol.* 8, 986:1-9.
 39. Issa R.M., El-Arousy M.H., Abd EI-Aal A.A.; Albendazole: A study of its effect on experimental *Trichinella spiralis* infection in rats, *Egypt. J. Med. Sci.* 19, 281-90 (1998).
 40. Ashour D.S., Abou Rayia D.M., Saad A.E., El- Bakary R.H.; Nitazoxanide anthelmintic activity against the enteral and parenteral phases of trichinellosis in experimentally infected rats, *Exp. Parasitol*, 170, 28-35 (2016).
 41. Dyab AK, Ahmed MA and Abdelazeem AG (2019) Prevalence and histopathology of *Trichinella spiralis* larvae of slaughtered pigs in Cairo governorate, Egypt. *Journal of the Egyptian Society of Parasitology* 49, 439–442.
 42. Bruschi F and Murrell KD (2002) New aspects of human trichinellosis: the impact of new *Trichinella* species. *Postgraduate Medical Journal* 78, 15–22.
 43. Kapel CM, Webster P and Gamble HR (2005) Muscle distribution of sylvatic and domestic *Trichinella* larvae in production animals and wildlife. *Veterinary Parasitology* 132, 101–105.
 44. Nassef N.E., El-Sobky M.M. and Afifi A.F.; Worm and larval burden, histopathological and ultrastructural evaluation of *T. spiralis* vaccination using crude worms and/or larvae antigens, *Experimental studies. PUJ*, 3; 27-38 (2010).
 45. MacManus J.F.A. and Mowry R.W.; Staining: *Histological and Histochemical*, 1st ed. Harper and Row, New York, USA, 74, 126 (1964).
 46. Priotti J., Codina A.V., Leonardi D., Vasconi M.D., Hinrichsen L.I., et al.; Albendazole microcrystal formulations based on chitosan and cellulose derivatives: physicochemical characterization and in vitro parasitocidal activity in *Trichinella spiralis* adult worms, *AAPS. Pharm. Sci. Tech.* ,18, 4, 947-56 (2017).
 47. Solana H., Scarella S., Virkel G., Ceriani C., Rodriguez J., et al.; Albendazole antiemetic metabolism and binding to cytosolic proteins in the liver fluke *Fasciola hepatica*, *Vet. Res. Commun*, 33, 2, 163-73 (2009).
 48. Abu El Ezz N.M.; Effect of *Nigella sativa* and *Allium cepa* oils on *Trichinella spiralis* in experimentally infected rats, *J Egypt Soc Parasitol*, 35, 511-523 (2005).
 49. Caner A., Döşkaya M., Değirmenci A., Can H., Baykan S., Uner A., Başdemir G., Zeybek U. and Gürüz Y.; Comparison of the effects of *Artemisia vulgaris* and *Artemisia absinthium* growing in western Anatolia against trichinellosis (*Trichinella spiralis*) in rats, *Exp Parasitol* ,119, 173-179 (2008).
 50. Shalaby M.A., Moghazy F.M., Shalaby H.A., Nasr S.M.; Effect of methanolic extract of *Balanites aegyptiaca* fruits on enteral and parenteral stages of *Trichinella spiralis* in rats, *Parasitol Res* ,107, 17-25 (2010).
 51. Abdel-Latif M., El-Shahawi G., Abolhadid S.M. and Abdel-Tawab H.; Immunoprotective effect of chitosan particles on *Hymenolepis nana*- infected mice. *Scand. J. Immunol.* 86, 2; 83-90 (2017).
 52. Gaafar M.R., Mady R.F., Diab R.G. and Shalaby T.I.; Chitosan and silver nanoparticles: Promising anti-toxoplasma agents, *Exp. Parasitol*, 143, 30-8 (2014).
 53. Mazzarino, L., Neckel, G.L., Bubniak, L.D., Mazzucco, S., Santos-Silva, M. C., Borsali, R. and Lemos-Senna, L. (2015): Curcumin-Loaded Chitosan-Coated Nanoparticles as a New Approach for the Local Treatment of Oral Cavity Cancer. *15(1):781-91. doi: 10.1166/jnn.2015.9189.*
 54. Hafez, E.N.; El Hamed, W.F. The Efficacy of Citrus maxima Peels Aqueous Extract Against Cryptosporidiosis in Immunocompromised Mice. *Acta Parasitol.* 2021, 66, 638–653. <https://doi.org/10.1007/s11686-020-00315-x>
 55. Wu Z., Nagano I., Boonmars T. and Takahashi Y. ; Tumor necrosis factor receptor-mediated apoptosis in *Trichinella spiralis*-infected muscle cells, *Parasitology*, 131, 373-381 (2005).
 56. Steensberg A., van Hall G., Osada T., Sacchetti M., Saltin B., Klarlund Pedersen B.; Production of interleukin-6 in contracting human skeletal muscles can account for the exercise-induced increase in plasma interleukin-6, *J Physiol*, 529 (Pt1), 237-242 (2000).

57. Pedersen BK, Steensberg A, and Schjerling P. Muscle-derived interleukin-6: possible biological effects. *J Physiol*. 2001 Oct 15; 536(Pt 2): 329–337.
58. Munoz-Canoves P., Scheele C., Pedersen B.K., Serrano A.L.; Interleukin-6 myokine signaling in skeletal muscle: a double-edged sword? *FEBS J*. 280,4131-4148 (2013).
59. Mirpuri, J., and Yarovinsky, F. (2012). IL-6 signaling SOCS critical for IL-12 host response to *Toxoplasma gondii*. *Future Microbiol*. 7, 13–16. doi: 10.2217/fmb.11.147.
60. Castro, A. S., Alves, C. M., Angeloni, M. B., Gomes, A. O., Barbosa, B. F., Franco, P. S., et al. (2013). Trophoblast cells are able to regulate monocyte activity to control *Toxoplasma gondii* infection. *Placenta* 34, 240–247. doi: 10.1016/j.placenta.2012.12.006.
61. da Silva R. J., Gomes A. O., Franco P. S., Pereira A. S., Milian I. C. B., Ribeiro M., et al.; Enrofloxacin and Toltrazuril are able to reduce *Toxoplasma gondii* growth in human BeWo trophoblastic cells and villous explants from human third trimester pregnancy. *Front. Cell. Infect. Microbiol*, 26, 7–340 (2017).. doi: 10.3389/fcimb.2017.00340
62. Nahrevanian H. Involvement of nitric oxide and its up/down stream molecules in the immunity against parasitic infections. *Braz J Infect Dis* 2009; (6):440-8.
63. Alipour M, Adineh F, Mosatafavi H, Aminabadi A, Monirinasab H, Jafari M. Effect of chronic intraperitoneal aminoguanidine on memory and expression of bcl-2 family genes in diabetic rats. *Can J Physiol Pharmacol* 2016; (94): 669–75.
64. Muro A, Perez-Arellano J. Nitric Oxide and Respiratory Helminthic Diseases. *J Biomed Biotechnol* 2010; (10): 1-8.
65. Scharton-Kersten T, Yap G, Magram J, Sher A. Inducible nitric oxide is essential for host control of persistent but not acute infection with the intracellular pathogen *Toxoplasma gondii*. *J Exp Med* 1997; 185 (7):1261-1273.
66. Krohncke K, Fehsel K, Kolb-Bachofen V. Inducible nitric oxide synthase in human diseases. *Clin. Exp. Immunol* 1998; (113):147.
67. Schlüter D, Deckert-Schlüter M, Lorenz E, Meyer T, Röllinghoff M, Bogdan C. Inhibition of Inducible Nitric Oxide Synthase Exacerbates Chronic Cerebral Toxoplasmosis in *Toxoplasma gondii*-Susceptible C57BL/6 Mice But Does Not Reactivate the Latent Disease in *T. gondii*-Resistant BALB/c Mice. *J Immunol* 1999; 162 (6) 3512-3518.
68. Sies H. Strategies of antioxidant defense. *Eur J Biochem* 215:213–219 (1993).
69. Derda M, Hadas E Antioxidants and proteolytic enzymes in experimental trichinellosis. *Acta Parasitol* 45:356–361 (2000).
70. Atia A. F., Abokhalil N.A. , Sweed D.M., Moaz I.M. , And Abou Hussien N.M.; Curcumin Nanoparticles Versus Curcumin In Amelioration Of Inflammatory And Pathological Changes During The Migratory Phase Of Murine Trichinellosis, *J. Egypt. Soc. Parasitol. (JESP)*, 51(2), 239 – 256 (2021).
71. Park M., Kang Y., Jo J., Baek K., Yu H., Choi Y., Ock M.S., Cha H.; Effect of Muscle Strength by *Trichinella spiralis* Infection during Chronic Phase, *International Journal of Medical Sciences*, 15(8), 802-807 (2018).
72. Garcia A., Barrera M.G., Piccirilli G., Vasconi M.D., Di Masso R.J., et al; Novel albendazole formulations given during the intestinal phase of *Trichinella spiralis* infection reduce effectively parasitic muscle burden in mice, *Parasitol. Int.*, 62, 6,568-70 (2013).
73. Tsai, B.Y., 2008. Effect of peels of lemon, orange, and grapefruit against *Meloidogyne incognita*. *Plant Pathol. Bull.* 17, 195–201